HDAC1/2 Inhibitor Therapy Improves Multiple Organ Systems in Aged Mice

Alessandra Tammaro[1,*], Eileen G. Daniels[2,3,*], Iman M. Hu[2,3,*], Kelly C. 't Hart[2,3,4,5], Kim Reid[6], Rio P. Juni[4,5], Loes M. Butter[1], Goutham Vasam[6], Rashmi Kamble[2], Aldo Jongejan[7], Richard I. Aviv[8,9], Joris J.T.H. Roelofs[1,10], Eleonora Aronica[11], Reinier A. Boon[4,5], Keir J. Menzies[6], Riekelt H. Houtkooper[2,3,5#], Georges E. Janssens[2,3,#]

[1] Amsterdam UMC location University of Amsterdam, Department of Pathology, Amsterdam Infection & Immunity, Amsterdam, Netherlands
[2] Laboratory Genetic Metabolic Diseases, Amsterdam University Medical Centers, University of Amsterdam, Amsterdam, The Netherlands.
[3] Amsterdam Gastroenterology, Endocrinology and Metabolism Institute, Amsterdam University Medical Centers, Amsterdam, The Netherlands.
[4] Department of Physiology, Amsterdam UMC, Vrije Universiteit Amsterdam, Amsterdam, Netherlands.
[5] Amsterdam Cardiovascular Sciences, Amsterdam University Medical Centers, Amsterdam, The Netherlands.
[6] Department of Biology, University of Ottawa, Canada
[7] Deptartment of Epidemiology & Data Science (EDS), Bioinformatics Laboratory, Amsterdam UMC, University of Amsterdam, Amsterdam, The Netherlands.
[8] Department of Medical Imaging, The Ottawa Hospital, 1053 Carling Ave, Ottawa, ON K1Y 4E9, Canada.
[9] Department of Radiology, University of Ottawa, Ottawa, ON, Canada.
[10] Amsterdam Cardiovascular Sciences, Microcirculation, location AMC
[11] Department of (Neuro)Pathology, Amsterdam UMC, University of Amsterdam, Amsterdam Neuroscience, Amsterdam, The Netherlands .
*Equal contribution
#Correspondence:
G.E. Janssens: g.e.janssens@amsterdamumc.nl

ABSTRACT

Aging increases the risk of age-related diseases, imposing substantial healthcare and personal costs. Targeting fundamental aging mechanisms pharmacologically can promote healthy aging and reduce this disease susceptibility. In this work, we employed transcriptome-based drug screening to identify compounds emulating transcriptional-signatures of long-lived genetic interventions. We discovered compound 60 (Cmpd60), a selective histone deacetylase 1 and 2 (HDAC1/2) inhibitor, mimicking diverse longevity interventions. In extensive molecular, phenotypic, and bioinformatic assessments using various cell and aged mouse models, we found Cmpd60 treatment to improve age-related phenotypes in multiple organs. Cmpd60 reduces renal epithelial-mesenchymal transition and fibrosis in kidney, diminishes dementia-related gene expression in brain, and enhances cardiac contractility and relaxation for the heart. In sum, our two-week HDAC1/2 inhibitor treatment in aged mice establishes a multi-tissue, healthy aging intervention in mammals, holding promise for therapeutic translation to promote healthy aging in humans.

INTRODUCTION

Increased age in individuals is linked to increased age-related chronic disease[1]. Although aging was long considered a passive process, it is now recognized that the rate of aging can be regulated by so-called longevity pathways[2]. These pathways are diverse, and can include modulation of the insulin-signaling pathway (e.g. targeting insulin-like growth factor 1 (IGF1)[3], insulin-like growth factor 1 receptor (IGF1R)[4], or insulin receptor substrate 1 (INSR)[5]), by modulation of mitochondrial biology (e.g. overexpression of sirtuin 6 (SIRT6)[6]), or by improving DNA repair (e.g. overexpression of the mitotic checkpoint gene BUB1, improving genomic stability[7]). Accordingly, many of these genetic interventions influence defined hallmarks of aging, including genomic instability, telomere attrition, epigenetic alterations, a loss of proteostasis, deregulated nutrient sensing, mitochondrial dysfunction, cellular senescence, and stem cell exhaustion[2,8].

The body of evidence demonstrating genetic interventions that modulate healthy longevity offers the potential for pharmaceutical development targeting these pathways, with the hopes to improve health in the elderly. These pharmaceutical interventions, termed geroprotectors, as they protect the gerontological part of life, are increasingly being uncovered[9–12]. In light of this, a first major testing of one of these compounds is underway in humans with the diabetes drug metformin and the 'treating aging with metformin' (TAME) clinical trial[13], to determine the ability to decrease the incidence of age-related diseases in the elderly.

While there are multiple candidate geroprotectors in line for testing in humans[11], there is still a great need for second-generation geroprotectors that are more potent and better recapitulate the longevity benefits resulting from genetic interventions. To address this need and circumvent the inherent difficulties of screening for such molecules, which require identifying a proper screening marker, assay development, and chemical screening, our team has been pioneering transcriptome-based drug screening for longevity interventions. For example, our approaches have identified HSP90 inhibitors as proteostasis-inducing longevity interventions[12], identified longevity compounds with minimized probabilities of side effects in humans[14], identified the acetylcholine receptor as a target to activate the pro-longevity transcription factor FOXO3[15,16], and the antiretroviral zidovudine to activate the pro-longevity transcription factor ATF4[17]. In addition to our own work, *in silico* drug screening has been used to identify a novel treatment for metabolic disorder[18], identify mimetics for the calorie restriction longevity intervention[19], and in general, de-risk early-phase drug screening[20].

In the current work, we performed multiple *in silico* drug screens using transcriptional profiles of 2837 small molecules testing their ability to mimic known genetic longevity interventions. We identified one compound that was most commonly found to mimic the transcriptional profile of the genetic longevity interventions. This benzamide-based small molecule, termed compound 60 (Cmpd60; aka Merck60 or BRD 692), is a selective histone deacetylase 1 and 2 (HDAC1/2) inhibitor. Cmpd60 was previously shown to repress growth in certain hematologic malignancies *in vitro*[21] and *in vivo* to cross the blood-brain barrier to reduce anxiety in mice[22]. Here, we used a combination of molecular, phenotypic, and bioinformatic analyses in multiple disease cell models and mouse models for age-related disease to establish if Cmpd60 acts as a geroprotector. Indeed, we found that Cmpd60 treatment attenuates age-associated phenotypes across multiple organ systems, including the kidney, brain, and heart. This is in line with our finding that Cmpd60's transcriptional signature mimics diverse longevity interventions, and with other individual accounts of certain (pan or class-specific) HDAC inhibitors benefiting individual diseases[23]. Our work establishes for the first time specifically HDAC1/2 inhibition as a healthy aging intervention in mammals, further

demonstrates that a single molecule can have pleiotropic beneficial effects for healthy aging on multiple organ systems, and paves the way for the development of more potent geroprotective therapeutics in mammals capable of recapitulating the benefits of diverse known genetic longevity interventions.

RESULTS

In silico transcriptome screening for pharmaceuticals mimicking genetic longevity interventions

In order to identify small molecules that could recapitulate the benefits of multiple genetic longevity interventions, we consulted the GeneAge database, where we found 75 genetic interventions (i.e. either knockdown/outs or overexpressions), which have been documented to extend lifespan[24]. We next turned to the library of integrated network-based cellular signatures (LINCS), an online database and software suite containing mRNA signatures of both drug-treated and genetically perturbed human cell lines[25,26]. Cross-referencing our list of 75 genetic longevity interventions with genetic perturbation cell lines, we found transcriptional signatures were available in the LINCS database for 25 of these (Figure 1A). These 25 interventions, along with FOXO3 overexpression as recently described[15], were used to query the LINCS database consisting of high-certain transcriptomes of 2837 small molecules present in 8 core cell lines (PC3, VCAP, A375, HA1E, HCC515, HT29, MCF7, and HEPG2), and identify those whose transcriptomic signatures were most similar to at least one of the genetic longevity intervention's transcriptomes (LINCS score > 90). To ensure the highest likelihood that our drug list would indeed benefit the aging process, we imposed a filter on the query, requiring that a drug's known target must also be included as a genetic perturbation hit. This resulted in 498 compounds mimicking at least one genetic longevity intervention (Figure 1A). Finally, drugs were ranked according to the number of genetic longevity interventions they transcriptionally mimicked, to form a prioritization ranking (Figure 1B).

When exploring the ranked list of drugs mimicking the most longevity interventions, we noted many well studied drugs in the context of aging (Figure S1). For example, the 3rd ranking drug, mimicking 10 out of the 25 genetic interventions, was sirolimus, well-known to extend lifespan in diverse model organisms[27]. Furthermore, ranked 4th and 5th included other molecules that extend lifespan in *C. elegans*, including digoxin[28], taxifolin[29], genestein[30], and catechin[31]. Indeed, many top ranked small molecules from our screen either extend lifespan in model organisms, or have other direct links to age-related pathways (Figure S1). However, the top ranked compound, which is the only one to bear transcriptional similarity to 12 out of the 25 genetic longevity interventions, was termed ''compound 60' (Cmpd60, or 'Merck60'), and had not yet been explored in the context of healthy aging (Figure 1B).

Cmpd60 is a benzamide-based small molecule that selectively inhibits histone deacetylase 1 and 2 (HDAC1/2). Interestingly, Cmpd60 mimicked the effects of the metabolic related genetic longevity interventions including knockdown of AKT (AKT^{KD}), and knockdown of multiple components of the insulin signalling pathway including $INSR^{KD}$ and $IRS1^{KD}$ (Figure 1B), in line with reports that pan-HDAC inhbition can prevent insulin resistance and obestiy in mice fed a high fat diet[32]. Furthermore, since HDAC inhibitors as a drug class may harbor some of the most promising geroprotective compounds[23], we believed Cmpd60 was an intruiging molecule to further explore in the context of geroprotection.

Cmpd60 in aged mice restores youthful molecular and physiological renal parameters

In order to investigate Cmpd60's potential protective effects during aging, we first turned to an *in vitro* model of renal fibrosis, a hallmark of age-related kidney disease. During aging, senescent tubular epithelial cells (TECs) accumulate in the kidney[33], which produce a wide range of profibrotic mediators, such as transforming growth factor-beta (TGF-β)[34]. This profibrotic cytokine in turn affects TECs' phenotype, promoting a partial epithelial-mesenchymal transition (EMT), ultimately leading to renal fibrosis[35]. Partial EMT in TECs is marked by an increased expression of the mesenchymal gene Alpha Smooth Muscle actin (αSMA) and a decrease in Zonula occludens-1 (ZO-1) and E-cadherin[36,37]. Indeed, treating TECs with recombinant TGFβ was sufficient to significantly increase αSMA and reduce ZO-1 protein expression (Figure 2A). We then tested if Cmpd60 could prevent EMT in TECs. We used a dose of 1μM Cmpd60, which is a non-toxic dose (Figure S2A) that effectively increases histone acetylation levels at histone H3K18 and H4K8 (Figure S2B-C). Strikingly, Cmpd60 partially prevented EMT upon TGFβ stimulation, reducing αSMA and increasing ZO-1 and E-cadherin protein expression (Figure 2A and Figure S2D).

To determine Cmpd60's geroprotective effects on the kidney at the molecular and physiological levels, we proceeded to treat aged male mice (20 months old) via intraperitoneal injection for 14 days with either Cmpd60 (22.5mg/kg) or control (Figure 2B). This dosing regimen was based in part on previous studies with Cmpd60[22]. EchoMRI measurements showed that fat mass, lean mass, and total body weight did not change between treated and untreated mice suggesting that Cmpd60 was tolerated at the dose used (Figure S2E), which matched the observation that blood biochemistry markers for renal and liver toxicity did not differ between the two groups (Figure S2F). Assessing acetylation levels revealed an increase of H4K8 acetylation in Cmpd60 treated kidneys, demonstrating efficacy of the intervention (Figure 2C, Figure S2G).

To assess the molecular effects of Cmpd60 on the kidney, we performed RNAseq transcriptomics on kidneys from the treated and untreated aged mice (Supplemental Table 1). Samples could be readily differentiated using partial least squares discriminant analysis (PLS-DA) (Figure 2D). Exploring the data further, we calculated differential expression between the groups, where we noted that inhibition of HDAC1/2 with Cmpd60 imparted clear differences on the transcriptional landscape ($p<0.01$, Supplemental Table 1). To better understand what these changes were, we performed gene ontology (GO) term and KEGG pathway analyses on the up and down regulated genes (Figure 2E, Supplemental Table 2). Here we found the top upregulated go term was one often associated to longevity, healthy aging and oxidative stress protection, namely, glutathione metabolic processes[38] (Figure 2E). These genes included Glutathione S-Transferase genes (*Gstm1*, *Gsta3*, and *Gsta4*) (Figure S2H), an important family of detoxifying and cytoprotective enzymes crucial for longevity[39] and as protective mechanism against the development of renal fibrosis healthy aging and oxidative stress protection. Given the decrease in partial EMT observed in the *in vitro* model, we sought to assess how these molecular changes manifest themselves at the physiological level. We performed histological analysis of renal fibrosis by analyzing collagen content detected with picro sirius red. Markedly, we found that the aged Cmpd60 treated mice showed less age-related renal fibrosis than their untreated counterparts (Figure 2F-G). Taken together, these findings suggest Cmpd60 alters the transcriptional landscape in aged kidney cells, shifting it towards a profile protective from oxidative stress and conducive to a reduction of renal EMT and age-related kidney fibrosis.

Cmpd60 treatment protects against detrimental brain aging processes

Having seen clear benefits of Cmpd60 treatment to the aged renal system, and noting prior work of others that demonstrated Cmpd60's ability to cross the blood brain barrier[22], we inquired the effects of Cmpd60 on the aged brain. Assessing histone modification in the brain revealed increased acetylation levels (Figure 3A, Figure S3A). Establishing this, we proceeded to perform RNAseq transcriptomics on brains of treated and untreated aged mice (Supplemental Table 3). Here, PLS-DA readily separated the two groups (Figure 3B), and we applied the same cutoff as for the kidney to assess differential expression ($P<0.01$, Figure S3B). Interestingly, assessing enriched

GO terms and KEGG pathways revealed an alteration in oxidative phosphorylation processes, down regulated upon treatment (Figure 3C, Supplemental Table 4). Remarkably, the KEGG pathway of Alzheimer's was also downregulated upon Cmpd60 treatment (Figure 3C). This included genes also involved in oxidative phosphorylation such as the NADH:Ubiquinone Oxidoreductase Subunits (NDUFs) (Figure 3D), in line with the finding that decreasing mitochondrial capacity can reduce amyloid-β toxicity[40].

Observing this potential beneficial effect, we next asked if Cmpd60 treatment could help prevent neurological decline in a dementia model. To address this, we turned to the APPSWE-1349 mouse model, a transgenic mouse overexpressing an isoform of human Alzheimer beta-amyloid (βA), which shows clear signs of impaired spatial referencing at 9-10 months of age[41]. We proceeded to treat APPSWE-1349 mice and control littermates for 14 days with either Cmpd60 (22.5mg/kg) or control (Figure 3E). We used mice younger than those that show full physiological symptoms, aged 6-7 months, to ensure the greatest chance of intervening in the early, molecular-based processes that occur and contribute to βA accumulation and neurodegeneration. Likewise we focused on molecular readouts to assess efficacy. Performing RNAseq transcriptomics on brain of these mice (Supplemental Table 5) and PLS-DA, revealed a strong separation of the non-treated transgenic mice, but less separation of the Cmpd60 treated transgenic mice from the control littermate mice (Figure 3F). This suggested Cmpd60 treatment was shifting the transgenic mouse profile away from a disease profile towards a non-disease profile. Comparing the differential gene expression between the treated and untreated transgenic mice (Figure S3C) and performing GO term and KEGG pathway enrichments (Supplemental Table 6), revealed that Cmpd60 reduced ribosomal gene expression (Figure S3D), while increasing membrane potential, ion transport, and cognitive processes (Figure S3E), changes previously reported to be conducive to decreased dementia risk[42–44]. Taking into account all four groups, namely the transgenic and control mice, both untreated and treated, allowed for an analysis of gene expression changes that Cmpd60 induced, unique to the transgenic disease model. Here, relevant for Cmpd60's potential effects in dementia specifically, we found an up regulation of memory related GO terms (Figure 3G, Supplemental Table 6). Some of the differentially expressed genes in this category included *Pla22g6*[45], *Cx3cr1*[46], *Ncam1*[47,48], *Cyfip1*[49] (Figure 3H), genes whose expression have been shown to benefit cognitive processes.

Finally, to determine how these transcriptional changes may manifest at the physiological level, we performed histological analysis of brains from the transgenic mice, either Cmpd60 treated or untreated. While the mice we studied were younger than the age at which aggregates are clearly visible, we found suggestive evidence that pre-aggregates were less present in Cmpd60 treated mice. Specifically, 4 out of 7 untreated mice showed aggregates (57%), while only 2 out of 6 Cmpd60 treated mice showed aggregates (33%) (Figure S3F). Taken together, our findings suggest Cmpd60 modifies the brain transcriptional landscape in a manner protective against the brain aging changes and counter to dementia related processes.

Cmpd60 treatment improves cardiac function

Having noted Cmpd60's beneficial effects on the aged kidney and brain, with relevance for two serious and under-treated age-related dysfunctions of renal failure and dementia, we next inquired as to the effects of Cmpd60 on one of the organs most contributing to age-related death: the heart. Our initial analysis did not reveal significant acetylation changes in histone H3 or H4 (Figure SF4A-C). Nonetheless, to further explore Cmpd60's cardiac-related effects more deeply, we performed RNAseq transcriptomics on hearts from aged treated and untreated mice (Supplemental Table 7). Here we again observed samples to be readily distinguishable upon PLS-DA (Figure 4A).

Upon evaluating differential expression in the Cmpd60 treated versus untreated heart samples, we noted far greater transcriptional changes following Cmpd60 treatment in the heart compared to either the kidney or brain. Accordingly, we applied a stricter cut-off to assess differential expression (adjusted p-value < 0.05) (Figure 4B). Although we found fewer GO enrichments and KEGG pathways related to altered oxidative phosphorylation processes, strikingly, we found the top enriched GO terms were related to heart valve development, suggesting profound changes

influencing heart function may be occurring upon Cmpd60 treatment (Figure 4C, Supplemental Table 8). This upregulation included genes such as SMAD Family Member 6 (*Smad6*), ADAM Metallopeptidase With Thrombospondin Type 1 Motif 9 (*Adamts9*), and Elastin Microfibril Interfacer 1 (*Emilin1*), members of gene families who have all been linked to cardiovascular outcomes, with either deficiency proving detrimental or abundance proving beneficial[50–52] (Figure 4D).

Spurred by these promising findings, we turned to an *in vitro* assay of cardiac functioning. Here, we assessed contraction (percentage of sarcomere shortening) and relaxation (return velocity) in adult rat ventricular cardiomyocytes. Remarkably, and in line with our *in vivo* findings at the transcriptional level, we found Cmpd60 treated ventricular cardiomyocytes showed both an improved contraction and relaxation parameters (Figure 4E-F). Taken together, this suggests Cmpd60 treatment modifies the cardiac transcriptional level and manifests itself at the functional level to improve age-related cardiac outcomes.

A consensus model of Cmpd60's effects

Having identified tissue-specific benefits of Cmpd60, we next inquired whether a conserved expression profile existed amongst the different tissues of the treated mice. To accomplish this, we assessed the overlap of differentially expressed genes in the kidney (p-value<0.05), brain (p-value<0.05), or heart (adjusted p-value<0.05). We identified 41 genes upregulated (Figure 5A) and 30 genes downregulated (Figure 5B) in common between the three tissues following Cmpd60 treatment. Amongst these 71 genes, for example, were genes including upregulated *Mapk3*, *Tgm2*, and *Spns2*, and downregulated *Mrps28* and *Fzd8* (Figure 5C). Transcription factor analysis querying diverse motif databases revealed six motifs (transfac-pro-M00797, cisbp-M6275, swissregulon-hs-HIF1A.p2, transfac-pro-M00466, transfac-pro-M07043, homer-TACGTGCV-HIF-1a) associated with Hif1a target genes (Figure 5D), suggesting Cmpd60 treatment increases oxidative stress resistance, an observation in line with the main transcriptional changes observed in the kidney and brain. Taken together, our work suggests both tissue specific effects of Cmp60 treatment, such as *Gsta2/3/4* and *Gstp1/3* in the kidney, *Wnt5a* in the brain, and *Scx* and *Emilin1* in the heart, as well as common transcriptional changes shared between tissues, oriented around *Hif1a* target gene expression. Together, the cumulated effects of these molecular changes may result in the age-reversing qualities we observed following Cmpd60 treatment in old mice.

DISCUSSION

In this work, we used an *in silico* drug screening platform and identified a single molecule, the HDAC1 and HDAC2 inhibitor Cmpd60, which possessed transcriptional signatures mimicking diverse genetic longevity interventions. In line with this, Cmpd60 demonstrated distinct effects across multiple organ systems where it was able to attenuate age-related phenotypes. In the kidney, Cmpd60 treatment increased protective gene expression related to oxidative stress regulation and reduced fibrosis possibly via reduced partial EMT detected in *in vitro* studies. This is in line with several studies supporting the link between decreased oxidative stress and amelioration of renal fibrosis[53,54]. In the brain, Cmpd60 treatment showed transcriptional changes conducive to improved cognitive functioning and molecular indications of neuroprotection in both naturally aged brain and a dementia mouse model brain. In the heart, Cmpd60 resulted in cardiac remodeling related transcriptional changes and benefitted cardiomyocyte functioning.

With Cmpd60 demonstrating such diverse age-related benefits across multiple organs, a question remains as to how these effects are mediated. HDAC inhibition has previously been suggested to benefit health through a plethora of mechanisms, including FOXO3 activation[55], Klotho upregulation[56], or reversing age-related acetylation changes, amongst others[23]. Notably, these have all been explored in diverse models and organs. The likeliest answer therefore is that HDAC inhibition modifies a tissue-specific epigenetic landscape, creating beneficial tissue specific responses (Figure 5E). Since aging is accompanied by alterations in histone acetylation patterns and global loss of transcriptional control[57], one tantalizing possibility is that Cmpd60 reverses these

acetylation changes and attenuates the aging phenotype in a tissue specific manner. Our findings at the transcriptional level, including an upregulation of oxidative stress protection and alterations in metabolic gene expression, catered to each organ, support this idea. It remains to be seen how each organ achieved such benefits, and how these findings can further translate to benefit human health.

One remarkable occurence we noted is the beneficial effects of Cmpd60 treatment in cardiac tissue, despite the fact that no changes in histone acetylation levels were observed in this system. This suggests that Cmpd60's HDAC-targeting effects may not be responsible for the changes observed in the heart, and rather, that the effects of Cmpd60 in the heart may be either (i) indirect, e.g. systemic effects from another body system that cross talk with the heart, or (ii) affecting acetylation levels of proteins other than HDACs. This seems to be different compared to the changes we have observed in the kidney and brain where histone acetylation changes were clearly observed. Indeed, HDAC inhibitors in general have been hypothesized to benefit the aging process by targeting non-histone related proteins (as well as histones)[23], and Cmpd60 may also act through multiple mechanisms, again in a tissue specific manner. The heart may be an example of this in our study.

Further exploring the link between Cmpd60 and *Hif1a* would be of great interest. This is especially the case considering past studies that have demonstrated HDACs to activate *Hif1a*, which therefore implies that a general suppression of *Hif1a* results upon treatment with HDAC inhibitors[58]. Different HDACs and HDAC inhibitors may have different regulatory effects on *Hif1a*, depending on dose and cell line used[59]. Here, it should be noted that while our RNAseq and bioinformatic analyses have revealed a clear link beftween *Hif1a* and Cmpd60, further *in vitro* studies co-treating cells with Cmpd60 and an *Hif1a* inhibitor would be required to formalize this relationship. In our kidney cell model, we observed a rescue of markers associated with pEMT following treatment with both TGF-β and Cmpd60. This restoration is likely facilitated by the modulation of Hif-1α. Indeed previous research has illustrated a time-dependent increase in Hif-1α levels in proximal tubular epithelial cells exposed to TGF-β. Moreover, inhibiting Hif-1α effectively inhibits TGF-β-induced EMT and attenuates kidney fibrosis, which aligns with our findings[53,60]. Therefore, the connection between *Hif1a* and Cmp60 should be seen as a candidate mechanism, requiring formal validation, and it is likely that Cmpd60 may work through other means as well. Indeed, while our *Hif1a* analyses showed suppression of *Hif1a* related genes, it also demonstrated activation of other *Hif1a* regulated genes.

Limitations

Several limitations should be considered with our study. For example, our study design involved treating aged animals and assessing a final time-point after the treatment period for molecular and physiological changes. With this design, we did not assess aged mice before treatment, and we cannot discern whether or not Cmpd60 acted to (i) rejuvenate the aged animals or (ii) attenuate age related changes that developed during the treatment period. Because the treatment period was relatively short, it can be expected that most changes observed after the treatment were the result of a reversal of aging phenotypes. However, a follow up study where histology and RNAseq of aged animals prior to treatment are collected would be required to address this fully, as well as young control animals for comparisons. Furthermore, another limitation of our work may be that our initial drug screen using datasets from the Broad Institute included many cancerous cell lines[26]. While this approach has been used before—by ourselves and others—identifying compounds benefiting health through diverse mechanisms not related to cancer[18,61,62], it could theoretically produce a confounding factor. It would be interesting to see what other compounds may emerge from similar screens when cancerous cell lines are excluded. Nonetheless, our current screen performed in this study has functioned to identify Cmpd60 as a candidate compound capable of addressing multiple aging phenotypes, meriting further investigation in-of-itself.

Conclusion

As most studies on HDAC inhibitors focus on one specific tissue, our study is unique in that it looks

369 at the effects of HDAC inhibition in three different organs; kidney, brain and heart. This enabled us
370 to recognize an overlapping gene expression profile in all three tissues; associated with *Hif1a* target
371 genes. Although we identified tissue-specific benefits of Cmpd60, it should be noted that HDAC
372 inhibitors are also known for their undesirable side effects[63]. Despite of, or thanks to, their many
373 diverse on- and off- target effects, HDAC inhibitors nonetheless benefit a range of preclinical age-
374 related disease models[23]. We therefore recommend future research to assess dose-dependent
375 effects of HDAC1/HDAC2 inhibitors in multiple organs.

Acknowledgements
AT is financially supported by the NWO-FAPESP joint grant on healthy ageing, executed by ZonMw (no. 457002002). GEJ is supported by a VENI grant from ZonMw, and AGEM Talent and Development grants. RHH is financially supported by an ERC Starting grant (no. 638290), a VIDI grant from ZonMw (no. 91715305) and by the Velux Stiftung (no. 1063). EGD is supported by a ZonMw travel grant (no. 446001023). MH is supported by a China Scholarship Council 2020 grant. EA is supported by, EU H2020- EpiEpiNet (No 952455).

Author Contributions
A.T., E.G.D., R.H.H. and G.E.J. conceived and designed the project. E.G.D. K.R., K.J.M. and R.I.A. organized and performed animal husbandry and Cmpd60 treatment and physiological animal measures. A.T. and L.M.B. performed kidney in vitro studies and with R.K. performed all biochemical analyses. A.T., E.A. and J.J.T.H.R. performed pathology analyses. A.J. and G.V. performed bioinformatics analyses. I.M.H. performed mouse transcriptomic analyses. K.C.H. R.P.J. and R.A.B. designed cardiac experiments and interpretations. A.T., E.G.D., R.H.H. and G.E.J. wrote the manuscript with contributions from all authors.

STAR methods

Key resource table

REAGENT or RESOURCE	SOURCE	IDENTIFIER
Antibodies		
Rabbit polyclonal anti-acetylated Histone H3 (Lys 18)	Cell Signaling	#9675
Rabbit polyclonal anti-total Histone 3	Cell Signaling	#9715
Rabbit polyclonal anti-acetylated Histone H4 (Lys8)	Cell Signaling	#2594
Rabbit polyclonal anti-total Histone H4	Cell Signaling	#2592
Mouse monoclonal anti-aSMA	Dako	#M085101
Rabbit polyclonal anti-ZO-1	Invitrogen	#617300
Mouse monoclonal anti- β-actin	Millipore	#MABT825
Rabbit monoclonal anti-GAPDH	Cell Signaling	#2118
Goat polyclonal anti rabbit-HRP	Dako	#P0448
Goat polyclonal anti msIgG2a-HRP	Southern Biotech	#1080-05
Goat polyclonal anti msIgG1-HRP	Southern Biotech	#1070-05
Chemicals, Peptides, and Recombinant Proteins		
Cmpd60, also known as Merck60. Broad Institute ID number BRD6929 and CAS No.: 849234-64-6	ChemShuttle	# 151025
TGF-β human recombinant	Prospec	#CYT-716
MTT	Sigma Aldrich	#M2128
Critical Commercial Assays		
RNeasy Mini Kit	Qiagen	#69504
Deposited Data		
RNA sequencing murine kidney, brain and heart	https://www.ncbi.nlm.nih.gov/geo/	#GSE247457
Experimental Models: Cell Lines		
Murine Immortalized proximal tubular epithelial cells (TECs)	Laboratory of Sandrine Florquin	N/A
Experimental Models: Organisms/Strains		
Aged BL6J males (age 78 weeks on arrival)	The Jackson Laboratory	Aged C57BL/6J Mice | The Jackson Laboratory (jax.org)

Male APPSWE-1349-RDI (Tg2756) tg/wt mice	Taconic	Model 1349
Male wistar rats	Charles River	NA
Software and Algorithms		
Image J	National Institute of health	https://imagej.nih.gov
GraphPad Prism (version 9.5.1)	GraphPad	https://www.graphpad.com
R (version 4.1.1)	R Foundation for statistical computing	https://www.r-project.org

Resource availability

Lead Contact:

Further information and requests for resources and reagents should be directed to and will be fulfilled by the Lead Contact, Georges E. Janssens (g.e.janssens@amsterdamumc.nl)

Materials availability

All unique/stable reagents generated in this study are available from the Lead Contact with a completed Materials Transfer Agreement.

Data and code availability

- Data generated from the bulk RNA-sequencing were uploaded to GEO and can be accessed with accession number GSE247457.
- This paper does not report original code
- Any additional information required to reanalyze the data reported in this paper is available from the lead contact upon request

Experimental model and study participant details

Mice

Animal studies were approved by the Institutional Animal Care and Veterinary Services from uOttawa, permit No. 2727.

Aged mice: Natural aged, approx. 20 months old, male BL6 mice were acquired from Taconic and single housed under a 12:12-hour light-dark cycle in a room set to 23°C (+/- 0.2°C). All animals were fed a regular chow diet. Mice received daily i.p. injections with either Cmpd60 (n=6) or vehicle (n=7) for 14 days total. Body weight was monitored every 5 days to adjust i.p. volumes to body weight. Cmpd60 treated animals received a dose of 22.5 mg/kg with an i.p. volume of 7.5 ml/kg. Cmpd60 was dissolved in 2% DMSO, 49% PEG400, and 49% saline solution (= vehicle) resulting in a 3 mg/ml concentration.

APPSWE-1349 mice: The APPSWE-1349 mice[64] (BL6 background) were acquired from Taconic. The transgenic mice possess a transgene coding for the 695-amino acid isoform of human Alzheimer β-amyloid (Aβ) precursor protein carrying the Swedish mutation. Animals (~6-7 months old) were single housed under a 12:12-hour light-dark cycle in a room set to 23°C (+/- 0.2°C). All animals were fed a regular chow diet. Mice received daily i.p. injections with either Cmpd60 (n=12) or vehicle (n=12) for 14 days total. Body weight was monitored every 5 days to adjust i.p. volumes to body weight. Cmpd60 treated animals received a dose of 22.5 mg/kg with an i.p. volume of 7.5 ml/kg. Cmpd60 was dissolved in 2% DMSO, 49% PEG400, and 49% saline solution (= vehicle) resulting in a 3 mg/ml concentration. On day 15, following 14 days of Cmpd60 treatment, mice (total body mass) were weighed and loaded into the Echo-MRI (EchoMRI-700 Analyzer) using an A100 antenna insert and then whole-body fat and lean mass were measured. Mice then underwent an

444 overnight fast (10 hours) and then were euthanized using CO_2, total body weight was determined,
445 followed by exsanguination through cardiac puncture. Blood (600-1000ml) was collected by cardiac
446 puncture into a heparin-coated syringes. Blood samples were centrifuged for 20 min at 4°C and the
447 separated plasma was stored at -80°C for further analysis. Tissues and organs were collected,
448 weighed and either snap frozen in liquid nitrogen or submerged in O.C.T. (Fisher Scientific) and
449 stored at -80°C.
450
451 For the plasma biochemical analysis**, r**enal, liver and body toxicity were determined by measuring
452 plasma levels of urea, creatinine, Aspartate aminotransferase (ASAT), Alanine transaminase
453 (ALAT) and Lactate Dehydrogenase (LDH). These parameters were determined by enzyme
454 reactions using standard autoanalyzer methods by our hospital research services.
455
456
457 **Method Details**
458
459 *In silico compound screen*
460 The online library of integrated network-based cellular signatures (LINCS)25,26 was accessed in
461 September 2017 through the cloud-based software platform CLUE (https://clue.io/). The
462 'touchstone' core dataset consisting of transcriptome signatures of eight cell lines (PC3, VCAP,
463 A375, HA1E, HCC515, HT29, MCF7, HEPG2) of 2837 different small molecule treatments, 3799
464 different gene knock-downs, and 2160 different gene overexpressions was used. From the gene
465 knock-downs or overexpression datasets, those genetic longevity interventions known to confer
466 lifespan extension in mouse models were used, (accessed in 2017 from GeneAge, filtering for
467 significant, positive lifespan effects in mice24). Individual queries were performed for each genetic
468 longevity intervention, producing lists of compounds with similar transcriptional signatures.
469 Compound lists were ranked and included a summary score consolidating cell line data, ranging
470 from −100 (opposing the genetic longevity signature) to 100 (mimicking the genetic longevity
471 signature). These were downloaded as.gct files (version 1.3). A cutoff was applied to the ranked
472 list such that compounds with a score > 90 were considered to match the transcriptional signature
473 of a longevity intervention. Drug lists were further filtered, such that a drug was only included as a
474 hit, if its drug target (i.e. the knockdown of the drug target) also passed a summary score cutoff >90
475 for the genetic longevity intervention in question. The final ranking was producing by tallying the
476 total number of genetic longevity interventions a compound could mimic (theoretical total 25), where
477 more than one compound could reach the same rank. Only one compound reached the top rank
478 (12 out of 25), Cmpd60.
479 Cmpd60, also known as Merck60 with Broad Institute ID number BRD6929 and CAS No.: 849234-
480 64-6 was acquired from ChemShuttle (USA, China), Catalog No.: 151025.
481
482
483 *RNA sequencing: Isolation of mRNA, library preparation and read mapping*
484 Mouse tissues were homogenized with a 5 mm steel bead using a TissueLyser II (QIAGEN) for 5
485 min at frequency of 30 times/second. RNA was extracted according to the instructions of the
486 RNaesy Mini Kit (QIAGEN). Contaminating genomic DNA was removed using RNase-Free DNase
487 (QIAGEN). RNA was quantified with a NanoDrop 2000 spectrophotometer (Thermo Scientific;
488 Breda, The Netherlands) and stored at -80°C until use.
489 RNA libraries were prepared and sequenced with the Illumina platform by Genome Scan (Leiden,
490 The Netherlands). The NEBNext Ultra II Directional RNA Library Prep Kit for Illumina was used to
491 process the sample(s). The sample preparation was performed according to the protocol "NEBNext
492 Ultra II Directional RNA Library Prep Kit for Illumina" (NEB #E7760S/L). Briefly, mRNA was isolated
493 from total RNA using the oligo-dT magnetic beads. After fragmentation of the mRNA, cDNA
494 synthesis was performed. This was used for ligation with the sequencing adapters and PCR
495 amplification of the resulting product. The quality and yield after sample preparation was measured
496 with the Fragment Analyzer. The size of the resulting products was consistent with the expected
497 size distribution (a broad peak between 300-500 bp). Clustering and DNA sequencing using the
498 NovaSeq6000 was performed according to manufacturer's protocols. A concentration of 1.1 nM of
499 DNA was used. NovaSeq control software NCS v1.6 was used.

Reads were subjected to quality control FastQC[65] trimmed using Trimmomatic v0.32 (Bolger et al., 2014) and aligned using HISAT2 v2.1.0 (Kim et al., 2015). Counts were obtained using HTSeq (v0.11.0, default parameters) (Anders et al., 2015) using the corresponding GTF taking into account the directions of the reads.

Transcriptome analysis and visualization

Data processing was performed using R version 4.1.1. Genes were reannotated using the Ensembl genome database and the biomaRt package[69]**.** Resulting p-values were corrected for multiple testing using the Benjamini–Hochberg false discovery rate where applicable. Biological process (BP) overrepresentation analysis was performed using Clusterprofiler 4.0.5[70] and org.Mm.eg.db (version 3.13.0). Gene selection (for figures 2E, 3C, 3G, 4C, supplementary figure 3D, 3E) was done based on p-value less than 0.01, and log Fold change larger than 0 for up-regulated genes, smaller than 0 for down-regulated genes. Partial least squares discriminant analysis (PLS-DA) was performed on normalized cpm value (genes with zero expression were filtered out) using MixOmics version 6.16.3[71]. Upset plots were generated using UpsetR version 1.4.0[72]. For transcription factor (TF) binding motif over-represention, analysis was performed using RcisTarget 1.14.0[73]. Shared up-regulated genes (pvalue < 0.05, log Fold change larger than 0) between brain, kidney and heart were used as input gene list. The same was performed for shared down-regulated genes. The following file (mm9-500bp-upstream-7species.mc9nr.feather) was used to specify the gene-motif rankings. “motifAnnotations_mgi_v9 ” was used for motif annotation to transcription factors. Additionally, the pheatmap (1.0.12), igraph (1.30) and ggplot2 (version 3.4.2) packages were used to generate heatmaps and various visualizations using colors from RcolorBrewer[74–76].

Histology and Immunostaining

Paraffin-embedded kidney and brain tissues were processed for (immuno)histological analysis. To quantify the percentage of interstitial fibrosis, Picro Sirius red histological staining was performed to detect collagen content. Kidney tissue slides were incubated with 0.2% Picro Sirius Red (PSR) solution (pH 2.0) for 1h followed by incubation with 0.01M HCl. The amount of PSR-positive staining per high power field (20x magnification) was quantified by Image J software. Beta amyloid plaques in brain slides were identified with beta Amyloid (1-42) antibody (Genetex: GTX134510). Quantification of the percentage of amyloid plaques was performed by the neuropathologist in a blinded manner

In vitro experiments

Murine Immortalized proximal tubular epithelial cells (TECs) were generated in Sandrine Florquin’s lab and cultured in DMEM/HAM F12 (Gibco) supplemented with 10% fetal calf serum, penicillin/streptomycin, 2mM L-glutamin (Invitrogen), 5µg/ml insulin (Gibco), 5µg/ml transferrin (Gibco), 5ng/ml selenite (Gibco), 40pg/ml Tri-iodo-thyrionine (Sigma), 36ng/ml hydrocortisone (Sigma) and 20ng/ml EGF (Sigma). TECs were maintained in culture at 33°C in medium supplemented with 10ng/ml IFNγ (Prospec) to maintain SV40 expression. One week before experiments were performed, TECs were differentiated at 37°C for 7 days in presence of complete medium without IFNγ. TECs were stimulated with 20ng/ml murine recombinant TGFβ (Prospec) for 72 hours in DMEM/F12 supplemented with 10% fetal calf serum, penicillin/streptomycin and 2mM L-glutamin. Cmpd60 was added either together with TGFβ for 72 hours or added in the last 6 hours of the experiment. After 72hrs cells were washed with PBS and processed for protein isolation.

Cell and tissue lysates and immunoblot

Cell lysates: RIPA lysis buffer (50mM Tris pH7.5, 0,15M NaCl 2mM EDTA, 1% deoxycholic acid, 1% nonidet P40, 0,1% SDS supplemented with 4mM Na3VO4, 0,5mM NaF and protease inhibitors (Sigma)) was added to the cells at the end of the experiment. Cells lysates were centrifuged and protein concentration was measured using a BCA assay kit (Thermo Scientific).

Tissue lysates: Freeze dried tissues (kidney, brain and heart) were homogenized in lysisbuffer (120mM Tris pH 6.8, 4% SDS, 20% glycerol supplemented with protease inhibitors) and stored overnight at -20C. The next day the homogenates were passed through a 21G needle and protein was measured using a BCA kit (Thermo Scientific).

556
557 Twenty µg of protein was loaded onto a 4-12% Bis-Tris gradient gel (Invitrogen) and separated
558 proteins were transferred on PVDF membrane (Millipore). After blocking aspecific signal,
559 membranes were incubated overnight at 4°C with primary antibodies listed in KRT. The following
560 day membranes were incubated with horseradish peroxidase (HRP)-conjugated secondary
561 antibodies for 1 hour at RT. Detection was done by ECL western blotting substrate (Thermo
562 Scientific) and images were obtained on a LAS 4000 (ImageQuant). Band intensity was quantified
563 through ImageJ.
564
565 *Adult rat ventricular cardiomyocyte isolation and contractility measurement.*
566 The animal experiments were performed in accordance with the guidelines from the Directive
567 2010/63/EU of the European Parliament on the protection of animals used for scientific purposes
568 and approved by the ethics committees of Amsterdam University Medical Centers, VUMC location,
569 Amsterdam, the Netherlands. Adult rat left ventricular cardiomyocytes (CMs) were isolated as
570 described previously[77,78]. Briefly, adult wild-type Wistar rats were terminated under anesthesia,
571 followed by chest opening and heart extraction. The heart was cannulated through the aorta and
572 perfused on a Langendorf perfusion set-up with liberase enzyme solution until the tissue was
573 sufficiently digested. The atria and right ventricle were removed and the left ventricle was minced
574 into small pieces and triturated. Subsequently, the cell suspension was filtered and re-suspended
575 in $CaCl_2$ buffers of increasing Ca^{2+} concentrations to reach a final concentration of 1mM. The
576 isolated adult CMs were finally re-suspended in plating medium containing Medium 199 (Lonza,
577 BE12-117F), 1% penicillin/streptomycin (Lonza, DE17-602DE) and 5% fetal bovine serum (PAA,
578 A15-101), and seeded on 1% laminin (L2020-1MG, Sigma)-coated plates (24-well format Costar
579 culture plate, Corning, 3524). One hour after plating, the medium was refreshed with maintenance
580 medium containing Medium 199, 1% penicillin/streptomycin and Insulin-Transferrin-Sodium
581 Selenite Supplement (Sigma-Aldrich; insulin, 10 mg l−1; transferrin, 5.5 mg l−1; and selenium
582 5µgl−1). Subsequently, the cells were stimulated with 5µM Cmpd60 (or corresponding vehicle,
583 DMSO) for 2 hours at 37°C in humidified air with 5% CO_2. After the stimulation, the contraction and
584 relaxation of the CMs were measured with the MultiCell microscope system (CytoCypher,
585 Amsterdam, the Netherlands) coupled to the Ionoptix high-speed sarcomere length measuring
586 software (Ionoptix LLC, Westwood, Massachusetts). Unloaded intact rat CMs were monitored
587 following field stimulation, and sarcomere shortening was measured and analyzed with the
588 automated, batch analysis software transient analysis tools (Cytosolver, CytoCypher) to determine
589 the contraction and relaxation profiles of the cells.
590
591 **Quantification and Statistical analysis**
592
593 *RNA seq*
594 Statistical analyses were performed using the edgeR v3.26.8 (Robinson et al., 2010) and
595 limma/voom v 3.40.6 [80] R packages. All genes with more than 2 counts in at least 3 of the samples
596 were kept. Count data were transformed to log2-counts per million (logCPM), normalized by
597 applying the trimmed mean of M-values method [79] and precision weighted using voom (Law et. al.,
598 2014). Differential expression was assessed using an empirical Bayes moderated t test within
599 limma's linear model framework including the precision weights estimated by voom [80,81]. Resulting
600 *p* values were corrected for multiple testing using the Benjamini-Hochberg false discovery rate.
601 Data processing was performed using R v3.6.1 and Bioconductor v3.9. Partial least-squares
602 discriminant analysis (PLS-DA) was performed using mixomics (Rohart et al., 2017) setting a
603 variable of importance (VIP) score of greater than 1 as significant. Resulting *p* values (where
604 applicable) were corrected for multiple testing using the Benjamini-Hochberg false discovery rate.
605 Genes were re-annotated using biomaRt using the Ensembl genome databases (v91).
606
607 *In vivo and in vitro assays*
608 Statistical analyses were performed using PRISM (9.5.1) and specific tests and corrections for
609 multiple hypothesis testing are listed in either each experiment's figure legend or corresponding
610 methods section.

611 **Figure legends**
612
613 **Figure 1 | Compound screen strategy and results to identify geroprotectors mimicking**
614 **genetic longevity interventions.** A) General outline of screening strategy. GeneAge database
615 was consulted for listing of genetic interventions, which were cross referenced against the LINCS
616 transcriptome database of cellular purturbations. Compounds best matching a genetic longevity
617 intevention at the transcriptional level were selected for further evaulation, and only those whose
618 drug targets were also present in knockdowns in the screen were included. This resulted in 498
619 compounds which were ranked based on how many different genetic longevity interventions their
620 transcriptional profiles could recapitulate. B) The top drugs ranked first (top, Cmpd60 as top-ranked
621 small molecule), to last (bottom) according to how many genetic interventions they mimick (blue
622 indicates a positive hit).
623
624 **Figure 2 | Influence of Cmpd60 on aging kidney**
625 A) Representative western blot of Tubular epithelial cells (TECs) treated with 20ng/ml of
626 recombinant TGFβ and with and without Cmpd60 (1 μM) for 72hrs. Protein lysates of TECs blotted
627 for anti-ZO-1, anti-E-cadherin, anti-αSMA and β-actin. Cmpd60 suppresses markers for partial EMT,
628 a hallmark of age-related renal fibrosis (n=3)/group. B) Schematic of aged mouse treatment
629 regimen with Cmpd60 and analyses. C) Relative Histone H4 acetylation levels (H4K8Ac) assessed
630 by western blot in renal tissue of aged mice with and without Cmpd60 treatment. Protein expression
631 was normalized against H4 total and expressed as mean ±SEM. Mann Whitney test was used to
632 determine statistical differences, **P<0.01. (n=5-6)/group. D) PLS-DA analysis of aged mice
633 treated with and without Cmpd60 (n=5-6)/group. E) Top GO terms of upregulated processes in
634 aged mice treated with Cmpd60 (see also Supplemental Table 2). F) Representative histological
635 images of Picro Sirius Red staining in kidney of aged mice with and without Cmp60. (n=5-6)/group.
636 G) Quantification of interstitial fibrosis determined by the percentage of positive Picro Sirius Red
637 staining/high power field, in mice treated with and without Cmpd60. Percentage of positive staining
638 was assessed with Image J software. Data are expressed as mean ±SEM and the Mann Whitney
639 test was used to determine statistical significance, *P<0.05, (n=5-6)/group
640
641 **Figure 3 | Cmpd60 treatment supports healthy brain aging**
642 A) Relative expression of Histone H4 acetylation levels (H4k8Ac) assessed by western blot in brain
643 tissue of aged mice treated with control and Cmpd60. Protein expression was normalized against
644 H4 total and expressed as mean ±SEM. Mann Whitney t-test was used to determine statistical
645 differences, **P<0.01. n=5-6/group. B) PLS-DA of RNA-seq transcriptome comparing Cmpd60
646 treated and untreated brain, n = 6 per group. C) Downregulated KEGG terms resulting from
647 Cmpd60 treatment. D) Boxplot of counts per million (CPM) expression values of genes in Cmpd60
648 treated mouse brain from the GO term enrichment of Alzheimer Disease. Fill represents condition,
649 grey for control and blue for Cmpd60. E) Schematic of dementia mouse model and treatment. F)
650 PLS-DA of RNA-seq transcriptome comparing dementia mice, controls, treated and untreated. G)
651 Up Go terms of interaction between the 4 groups, revealing altered cognitive processes. H) Boxplot
652 of CPM expression values of genes from the GO term enrichment of cognition in (E). Fill represents
653 condition, grey for control and blue for Cmpd60.
654
655 **Figure 4 | Cmpd60 treatment benefits cardiac tissues.**
656 A) PLS-DA of RNAseq, aged heart, treated vs untreated (n = 5-6/group). B) Volcano plot of RNAseq
657 differential expression, aged heart, treated vs untreated (n = 5-6/group). Genes with p-value < 0.01
658 were colored (red: up-regulated, blue: down-regulated). C) Top GO Terms from upregulated genes.
659 D) Boxplot of CPM expression values of genes in Cmpd60 treated mouse heart from the GO term
660 enrichment of Heart Valve Development. E) Treatment of cardiomyocytes with Cmpd60 increased
661 contraction, as shown by increased % sarcomere shortening. F) Treatment of cardiomyocytes with
662 Cmpd60 improved relaxation, as assessed by higher return velocity (n=4, corresponding to 4
663 independent experiments; 30-40 CMs were measured per condition per experiment; data are
664 represented as mean ± SD, *p*<0.05, unpaired *t*-test).
665
666 **Figure 5 | A consensus model of Cmpd60's effects**

A) Comparison of the unique and shared upregulated genes in the three tissues; kidney, heart and brain. 41 genes are commonly upregulated in the three tissues (highlighted in blue) B) Comparison of the unique and shared downregulated genes in the three tissues. 30 genes are commonly downregulated in the three tissues (highlighted in blue) C) Heatmap of the log fold change of genes with shared regulation in three tissues (for visualization purposes, log fold changes exceeding 2 were capped at 2, while values below -2 were capped at -2). D) Network for transcription factor Hif1a, one of the top predicted TFs based on motif overrepresentation of the commonly changed genes among the three tissues. Squares represents different motifs annotated to Hif1a. Edges connect each motifs to the genes contributing to its enrichment. E) Model of Cmpd60's geroprotective effects, which are due to both tissue specific and conserved transcriptional changes, producing net aging-protective effects.

Declaration of interests

The authors declare no competing interests.

Inclusion and Diversity

We support inclusive, diverse and equitable conduct of research

Bibliography

1. Kennedy, B.K., Berger, S.L., Brunet, A., Campisi, J., Cuervo, A.M., Epel, E.S., Franceschi, C., Lithgow, G.J., Morimoto, R.I., Pessin, J.E., et al. (2014). Geroscience: Linking aging to chronic disease, 10.1016/j.cell.2014.10.039 10.1016/j.cell.2014.10.039.
2. López-Otín, C., Blasco, M.A., Partridge, L., Serrano, M., and Kroemer, G. (2013). The hallmarks of aging. Cell *153*. 10.1016/j.cell.2013.05.039.
3. Mao, K., Quipildor, G.F., Tabrizian, T., Novaj, A., Guan, F., Walters, R.O., Delahaye, F., Hubbard, G.B., Ikeno, Y., Ejima, K., et al. (2018). Late-life targeting of the IGF-1 receptor improves healthspan and lifespan in female mice. Nature Communications. 10.1038/s41467-018-04805-5.
4. Holzenberger, M., Dupont, J., Ducos, B., Leneuve, P., Géloën, A., Even, P.C., Cervera, P., and Le Bouc, Y. (2003). IGF-1 receptor regulates lifespan and resistance to oxidative stress in mice. Nature *421*, 182–187. 10.1038/nature01298.
5. Selman, C., Lingard, S., Choudhury, A.I., Batterham, R.L., Claret, M., Clements, M., Ramadani, F., Okkenhaug, K., Schuster, E., Blanc, E., et al. (2008). Evidence for lifespan extension and delayed age–related biomarkers in insulin receptor substrate 1 null mice. The FASEB Journal. 10.1096/fj.07-9261com.
6. Kanfi, Y., Naiman, S., Amir, G., Peshti, V., Zinman, G., Nahum, L., Bar-Joseph, Z., and Cohen, H.Y. (2012). The sirtuin SIRT6 regulates lifespan in male mice. Nature. 10.1038/nature10815.
7. Baker, D.J., Dawlaty, M.M., Wijshake, T., Jeganathan, K.B., Malureanu, L., Van Ree, J.H., Crespo-Diaz, R., Reyes, S., Seaburg, L., Shapiro, V., et al. (2013). Increased expression of BubR1 protects against aneuploidy and cancer and extends healthy lifespan. Nature Cell Biology. 10.1038/ncb2643.
8. van der Rijt, S., Molenaars, M., McIntyre, R.L., Janssens, G.E., and Houtkooper, R.H. (2020). Integrating the Hallmarks of Aging Throughout the Tree of Life: A Focus on Mitochondrial Dysfunction. Frontiers in Cell and Developmental Biology *8*, 1–12. 10.3389/fcell.2020.594416.
9. Moskalev, A., Chernyagina, E., Tsvetkov, V., Fedintsev, A., Shaposhnikov, M., Krut'ko, V., Zhavoronkov, A., and Kennedy, B.K. (2016). Developing criteria for evaluation of geroprotectors as a key stage toward translation to the clinic, 10.1111/acel.12463 10.1111/acel.12463.
10. Moskalev, A., Chernyagina, E., Kudryavtseva, A., and Shaposhnikov, M. (2017). Geroprotectors: A Unified Concept and Screening Approaches. Aging and disease *8*, 354. 10.14336/ad.2016.1022.

11. Partridge, L., Fuentealba, M., and Kennedy, B.K. (2020). The quest to slow ageing through drug discovery. Nature Reviews Drug Discovery *19*, 513–532. 10.1038/s41573-020-0067-7.
12. Janssens, G.E., Lin, X.X., Millan-Ariño, L., Kavšek, A., Sen, I., Seinstra, R.I., Stroustrup, N., Nollen, E.A.A., and Riedel, C.G. (2019). Transcriptomics-Based Screening Identifies Pharmacological Inhibition of Hsp90 as a Means to Defer Aging. Cell Reports *27*, 467-480.e6. 10.1016/j.celrep.2019.03.044.
13. Kulkarni, A.S., Gubbi, S., and Barzilai, N. (2020). Benefits of Metformin in Attenuating the Hallmarks of Aging. Cell Metabolism *32*, 15–30. 10.1016/J.CMET.2020.04.001.
14. Janssens, G.E., and Houtkooper, R.H. (2020). Identification of longevity compounds with minimized probabilities of side effects. Biogerontology *21*, 709–719. 10.1007/s10522-020-09887-7.
15. McIntyre, R.L., Denis, S.W., Kamble, R., Molenaars, M., Petr, M., Schomakers, B. V., Rahman, M., Gupta, S., Toth, M.L., Vanapalli, S.A., et al. (2021). Inhibition of the neuromuscular acetylcholine receptor with atracurium activates FOXO/DAF-16-induced longevity. Aging Cell *20*, 1–32. 10.1111/acel.13381.
16. McIntyre, R.L., Liu, Y.J., Hu, M., Morris, B.J., Willcox, B.J., Donlon, T.A., Houtkooper, R.H., and Janssens, G.E. (2022). Pharmaceutical and nutraceutical activation of FOXO3 for healthy longevity. Ageing Research Reviews *78*, 101621. 10.1016/j.arr.2022.101621.
17. McIntyre, R.L., Molenaars, M., Schomakers, B. V., Gao, A.W., Kamble, R., Jongejan, A., van Weeghel, M., van Kuilenburg, A.B.P., Possemato, R., Houtkooper, R.H., et al. (2023). Anti-retroviral treatment with zidovudine alters pyrimidine metabolism, reduces translation, and extends healthy longevity via ATF-4. Cell Reports *42*. 10.1016/j.celrep.2022.111928.
18. Liu, J., Lee, J., Hernandez, M.A.S., Mazitschek, R., and Ozcan, U. (2015). Treatment of obesity with celastrol. Cell *161*, 999–1011. 10.1016/j.cell.2015.05.011.
19. Calvert, S., Tacutu, R., Sharifi, S., Teixeira, R., Ghosh, P., and de Magalhães, J.P. (2016). A network pharmacology approach reveals new candidate caloric restriction mimetics in C. elegans. Aging Cell *15*, 256–266. 10.1111/acel.12432.
20. Verbist, B., Klambauer, G., Vervoort, L., Talloen, W., Shkedy, Z., Thas, O., Bender, A., Göhlmann, H.W.H., and Hochreiter, S. (2015). Using transcriptomics to guide lead optimization in drug discovery projects: Lessons learned from the QSTAR project, 10.1016/j.drudis.2014.12.014 10.1016/j.drudis.2014.12.014.
21. Stubbs, M.C., Kim, W., Bariteau, M., Davis, T., Vempati, S., Minehart, J., Witkin, M., Qi, J., Krivtsov, A. V., Bradner, J.E., et al. (2015). Selective inhibition of HDAC1 and HDAC2 as a potential therapeutic option for B-ALL. Clinical Cancer Research *21*, 2348–2358. 10.1158/1078-0432.CCR-14-1290.
22. Lewis, M.C., Fass, D.M., Wagner, F.F., Hennig, K.M., Gale, J., Hdac, A.S., Schroeder, F.A., Lewis, M.C., Fass, D.M., Wagner, F.F., et al. (2014). A Selective HDAC 1 / 2 Inhibitor Modulates Chromatin and Gene Expression in Brain and Alters Mouse Behavior in Two Mood-Related Tests. Plos One *8*, e71323 (1-11). 10.1371/journal.pone.0071323.
23. McIntyre, R.L., Daniels, E.G., Molenaars, M., Houtkooper, R.H., and Janssens, G.E. (2019). From molecular promise to preclinical results: HDAC inhibitors in the race for healthy aging drugs. EMBO Molecular Medicine *11*. 10.15252/emmm.201809854.
24. Tacutu, R., Thornton, D., Johnson, E., Budovsky, A., Barardo, Di., Craig, T., DIana, E., Lehmann, G., Toren, D., Wang, J., et al. (2018). Human Ageing Genomic Resources: New and updated databases. Nucleic Acids Research *46*, D1083–D1090. 10.1093/nar/gkx1042.
25. Keenan, A.B., Jenkins, S.L., Jagodnik, K.M., Koplev, S., He, E., Torre, D., Wang, Z., Dohlman, A.B., Silverstein, M.C., Lachmann, A., et al. (2018). The Library of Integrated Network-Based Cellular Signatures NIH Program: System-Level Cataloging of Human Cells Response to Perturbations, 10.1016/j.cels.2017.11.001 10.1016/j.cels.2017.11.001.
26. Subramanian, A., Narayan, R., Corsello, S.M., Peck, D.D., Natoli, T.E., Lu, X., Gould, J., Davis, J.F., Tubelli, A.A., Asiedu, J.K., et al. (2017). A Next Generation Connectivity Map: L1000 Platform and the First 1,000,000 Profiles. Cell *171*, 1437-1452.e17. 10.1016/j.cell.2017.10.049.
27. Johnson, S.C., Rabinovitch, P.S., and Kaeberlein, M. (2013). MTOR is a key modulator of

ageing and age-related disease. Nature *493*, 338–345. 10.1038/nature11861.

28. Wang, C., Niederstrasser, H., Douglas, P.M., Lin, R., Jaramillo, J., Li, Y., Olswald, N.W., Zhou, A., McMillan, E.A., Mendiratta, S., et al. (2017). Small-molecule TFEB pathway agonists that ameliorate metabolic syndrome in mice and extend C. elegans lifespan. Nature Communications. 10.1038/s41467-017-02332-3.
29. Benedetti, M.G., Foster, A.L., Vantipalli, M.C., White, M.P., Sampayo, J.N., Gill, M.S., Olsen, A., and Lithgow, G.J. (2008). Compounds that confer thermal stress resistance and extended lifespan. Experimental Gerontology. 10.1016/j.exger.2008.08.049.
30. Lee, E.B., Ahn, D., Kim, B.J., Lee, S.Y., Seo, H.W., Cha, Y.S., Jeon, H., Eun, J.S., Cha, D.S., and Kim, D.K. (2015). Genistein from vigna angularis extends lifespan in caenorhabditis elegans. Biomolecules and Therapeutics *23*, 77–83. 10.4062/biomolther.2014.075.
31. Saul, N., Pietsch, K., Menzel, R., Stürzenbaum, S.R., and Steinberg, C.E.W. (2009). Catechin induced longevity in C. elegans: From key regulator genes to disposable soma. Mechanisms of Ageing and Development. 10.1016/j.mad.2009.05.005.
32. Ye, J., Martin, R.J., Gao, Z., Zhang, J., Ward, R.E., Yin, J., Lefevre, M., and Cefalu, W.T. (2009). Butyrate Improves Insulin Sensitivity and Increases Energy Expenditure in Mice. Diabetes *58*, 1509–1517. 10.2337/db08-1637.
33. Valentijn, F.A., Falke, L.L., Nguyen, T.Q., and Goldschmeding, R. (2018). Cellular senescence in the aging and diseased kidney. Journal of cell communication and signaling *12*, 69–82. 10.1007/s12079-017-0434-2.
34. Luo, C., Zhou, S., Zhou, Z., Liu, Y., Yang, L., Liu, J., Zhang, Y., Li, H., Liu, Y., Hou, F.F., et al. (2018). Wnt9a promotes renal fibrosis by accelerating cellular senescence in tubular epithelial cells. Journal of the American Society of Nephrology. 10.1681/ASN.2017050574.
35. O'Sullivan, E.D., Hughes, J., and Ferenbach, D.A. (2017). Renal aging: Causes and consequences. Journal of the American Society of Nephrology *28*, 407–420. 10.1681/ASN.2015121308.
36. Lamouille, S., Xu, J., and Derynck, R. (2014). Molecular mechanisms of epithelial-mesenchymal transition. Nature reviews. Molecular cell biology *15*, 178–196. 10.1038/nrm3758.
37. Liu, Y. (2010). New insights into epithelial-mesenchymal transition in kidney fibrosis, 10.1681/ASN.2008121226 10.1681/ASN.2008121226.
38. Ahn, E., Lee, J., Han, J., Lee, S.M., Kwon, K.S., and Hwang, G.S. (2021). Glutathione is an aging-related metabolic signature in the mouse kidney. Aging. 10.18632/aging.203509.
39. Scarfò, M., Sciandra, C., Ruberto, S., and Santovito, A. (2021). GSTT1, GSTP1 and XPC genes are associated with longevity in an Italian cohort. Annals of Human Biology. 10.1080/03014460.2021.1985170.
40. Sorrentino, V., Romani, M., Mouchiroud, L., Beck, J.S., Zhang, H., D'Amico, D., Moullan, N., Potenza, F., Schmid, A.W., Rietsch, S., et al. (2017). Enhancing mitochondrial proteostasis reduces amyloid-β proteotoxicity. Nature. 10.1038/nature25143.
41. Hsiao, K., Chapman, P., Nilsen, S., Eckman, C., Harigaya, Y., Younkin, S., Yang, F., and Cole, G. (1996). Correlative memory deficits, Abeta elevation, and ... [Science. 1996] - PubMed result. Science (New York, N.Y.).
42. Sorrentino, V., Romani, M., Mouchiroud, L., Beck, J.S., Zhang, H., D'Amico, D., Moullan, N., Potenza, F., Schmid, A.W., Rietsch, S., et al. (2017). Enhancing mitochondrial proteostasis reduces amyloid-β proteotoxicity. Nature *552*, 187–193. 10.1038/nature25143.
43. Bottley, A., Phillips, N.M., Webb, T.E., Willis, A.E., and Spriggs, K.A. (2010). eIF4A inhibition allows translational regulation of mRNAs encoding proteins involved in Alzheimer's Disease. PLoS ONE. 10.1371/journal.pone.0013030.
44. Fabiani, C., and Antollini, S.S. (2019). Alzheimer's disease as a membrane disorder: Spatial cross-talk among beta-amyloid peptides, nicotinic acetylcholine receptors and lipid rafts, 10.3389/fncel.2019.00309 10.3389/fncel.2019.00309.
45. Miki, Y., Tanji, K., Mori, F., Kakita, A., Takahashi, H., and Wakabayashi, K. (2017). PLA2G6 accumulates in Lewy bodies in PARK14 and idiopathic Parkinson's disease.

Neuroscience Letters. 10.1016/j.neulet.2017.02.027.

46. Rogers, J.T., Morganti, J.M., Bachstetter, A.D., Hudson, C.E., Peters, M.M., Grimmig, B.A., Weeber, E.J., Bickford, P.C., and Gemma, C. (2011). CX3CR1 deficiency leads to impairment of hippocampal cognitive function and synaptic plasticity. Journal of Neuroscience. 10.1523/JNEUROSCI.3667-11.2011.

47. Chen, K., Gao, T., Bai, Z., and Yuan, Z. (2018). Circulating APP, NCAM and Aβ serve as biomarkers for Alzheimer's disease. Brain Research. 10.1016/j.brainres.2018.08.015.

48. Zhao, J., Lu, W., Li, J., Liu, L., and Zhao, X. (2021). Decreased Serum NCAM Levels Associated with Cognitive Impairment in Vascular Dementia. Disease Markers. 10.1155/2021/2792884.

49. San Segundo-Acosta, P., Montero-Calle, A., Jernbom-Falk, A., Alonso-Navarro, M., Pin, E., Andersson, E., Hellström, C., Sánchez-Martínez, M., Rábano, A., Solís-Fernández, G., et al. (2021). Multiomics Profiling of Alzheimer's Disease Serum for the Identification of Autoantibody Biomarkers. Journal of Proteome Research. 10.1021/acs.jproteome.1c00630.

50. Tan, H.L., Glen, E., Töpf, A., Hall, D., O'Sullivan, J.J., Sneddon, L., Wren, C., Avery, P., Lewis, R.J., ten Dijke, P., et al. (2012). Nonsynonymous variants in the SMAD6 gene predispose to congenital cardiovascular malformation. Human Mutation. 10.1002/humu.22030.

51. Santamaria, S., and de Groot, R. (2020). ADAMTS proteases in cardiovascular physiology and disease. Open Biology. 10.1098/rsob.200333.

52. Zanetti, M., Braghetta, P., Sabatelli, P., Mura, I., Doliana, R., Colombatti, A., Volpin, D., Bonaldo, P., and Bressan, G.M. (2004). EMILIN-1 Deficiency Induces Elastogenesis and Vascular Cell Defects. Molecular and Cellular Biology. 10.1128/mcb.24.2.638-650.2004.

53. Han, W.Q., Zhu, Q., Hu, J., Li, P.L., Zhang, F., and Li, N. (2013). Hypoxia-inducible factor prolyl-hydroxylase-2 mediates transforming growth factor beta 1-induced epithelial-mesenchymal transition in renal tubular cells. Biochimica et Biophysica Acta - Molecular Cell Research *1833*, 1454–1462. 10.1016/j.bbamcr.2013.02.029.

54. Marquez-Exposito, L., Tejedor-Santamaria, L., Valentijn, F.A., Tejera-Muñoz, A., Rayego-Mateos, S., Marchant, V., Rodrigues-Diez, R.R., Rubio-Soto, I., Knoppert, S.N., Ortiz, A., et al. (2022). Oxidative Stress and Cellular Senescence Are Involved in the Aging Kidney. Antioxidants *11*, 1–19. 10.3390/antiox11020301.

55. Shimazu, T., Hirschey, M.D., Newman, J., He, W., Shirakawa, K., Le Moan, N., Grueter, C.A., Lim, H., Saunders, L.R., Stevens, R.D., et al. (2013). Suppression of oxidative stress by β-hydroxybutyrate, an endogenous histone deacetylase inhibitor. Science *339*, 211–214. 10.1126/science.1227166.

56. Lin, W., Li, Y., Chen, F., Yin, S., Liu, Z., and Cao, W. (2017). Klotho preservation via histone deacetylase inhibition attenuates chronic kidney disease-associated bone injury in mice. Scientific Reports. 10.1038/srep46195.

57. Peleg, S., Feller, C., Ladurner, A.G., and Imhof, A. (2016). The Metabolic Impact on Histone Acetylation and Transcription in Ageing, 10.1016/j.tibs.2016.05.008 10.1016/j.tibs.2016.05.008.

58. Kim, S., Jeong, J., Park, J.A.E., Lee, J., Seo, J.I.H.A.E., Jung, B., Bae, M., and Kim, K. (2007). Regulation of the HIF-1α stability by histone deacetylases. Oncology Reports *17*, 647–651.

59. Tong, B.C.-K., and Benjamin Chun-Kit Tong (2017). Class I and IIa HDACs mediate HIF-1α stability through PHD2-dependent mechanism while HDAC6, a class IIb member, promotes HIF-1α transcriptional activity in nucleus pulposus cells of the intervertebral disc. Physiology & behavior *176*, 139–148. 10.1002/jbmr.2787.Class.

60. Zhao, H., Han, Y., Jiang, N., Li, C., Yang, M., Xiao, Y., Wei, L., Xiong, X., Yang, J., Tang, C., et al. (2021). Effects of HIF-1α on renal fibrosis in cisplatin-induced chronic kidney disease. Clinical Science *135*, 1273–1288. 10.1042/CS20210061.

61. McIntyre, R.L., Denis, S.W., Kamble, R., Molenaars, M., Petr, M., Schomakers, B. V., Rahman, M., Gupta, S., Toth, M.L., Vanapalli, S.A., et al. (2021). Inhibition of the neuromuscular acetylcholine receptor with atracurium activates FOXO/DAF-16-induced longevity. Aging Cell, 1–16. 10.1111/acel.13381.

62. Rebecca L. McIntyre, Marte Molenaars, Bauke V. Schomakers, and Georges E. Janssens Anti-retroviral treatment with zidovudine alters pyrimidine metabolism, reduces translation, and extends healthy longevity via ATF-4. Unpublished.
63. Yang, S. shuang, Zhang, R., Wang, G., and Zhang, Y. fang (2017). The development prospection of HDAC inhibitors as a potential therapeutic direction in Alzheimer's disease, 10.1186/s40035-017-0089-1 10.1186/s40035-017-0089-1.
64. Hsiao, K., Chapman, P., Nilsen, S., Eckman, C., Harigaya, Y., Younkin, S., Yang, F., and Cole, G. (1996). Correlative memory deficits, Aβ elevation, and amyloid plaques in transgenic mice. Science. 10.1126/science.274.5284.99.
65. Andrews, S., and others (2019). FastQC: a quality control tool for high throughput sequence data. 2010 at Babraham Bioinformatics, Babraham Institute.
66. Bolger, A.M., Lohse, M., and Usadel, B. (2014). Trimmomatic: a flexible trimmer for Illumina sequence data. Bioinformatics *30*, 2114–2120. 10.1093/bioinformatics/btu170.
67. Kim, D., Langmead, B., and Salzberg, S.L. (2015). HISAT: a fast spliced aligner with low memory requirements. Nature methods *12*, 357–360. 10.1038/nmeth.3317.
68. Anders, S., Pyl, P.T., and Huber, W. (2015). HTSeq—a Python framework to work with high-throughput sequencing data. Bioinformatics *31*, 166–169. 10.1093/bioinformatics/btu638.
69. Durinck, S., Spellman, P.T., Birney, E., and Huber, W. (2009). Mapping identifiers for the integration of genomic datasets with the R/Bioconductor package biomaRt. Nature Protocols *4*, 1184–1191. 10.1038/nprot.2009.97.
70. Wu, T., Hu, E., Xu, S., Chen, M., Guo, P., Dai, Z., Feng, T., Zhou, L., Tang, W., Zhan, L., et al. (2021). clusterProfiler 4.0: A universal enrichment tool for interpreting omics data. The Innovation. 10.1016/j.xinn.2021.100141.
71. Rohart, F., Gautier, B., Singh, A., and Lê Cao, K.-A. (2017). mixOmics: An R package for 'omics feature selection and multiple data integration. PLoS computational biology *13*, e1005752.
72. Conway, J.R., Lex, A., and Gehlenborg, N. (2017). UpSetR: An R package for the visualization of intersecting sets and their properties. Bioinformatics *33*, 2938–2940. 10.1093/bioinformatics/btx364.
73. Aibar, S., González-Blas, C.B., Moerman, T., Huynh-Thu, V.A., Imrichova, H., Hulselmans, G., Rambow, F., Marine, J.C., Geurts, P., Aerts, J., et al. (2017). SCENIC: Single-cell regulatory network inference and clustering. Nature Methods. 10.1038/nmeth.4463.
74. Wickham, H. (2016). ggplot2: elegant graphics for data analysis at Springer-Verlag.
75. Neuwirth, E. (2014). RColorBrewer: ColorBrewer palettes. R package version 1.1-2, https://cran.R-project.org/package=RColorBrewer.
76. Csardi, G., and Nepusz, T. (2006). The igraph software package for complex network research. InterJournal Complex Systems.
77. Juni, R.P., Kuster, D.W.D., Goebel, M., Helmes, M., Musters, R.J.P., van der Velden, J., Koolwijk, P., Paulus, W.J., and van Hinsbergh, V.W.M. (2019). Cardiac Microvascular Endothelial Enhancement of Cardiomyocyte Function Is Impaired by Inflammation and Restored by Empagliflozin. JACC: Basic to Translational Science. 10.1016/j.jacbts.2019.04.003.
78. Juni, R.P., Al-Shama, R., Kuster, D.W.D., van der Velden, J., Hamer, H.M., Vervloet, M.G., Eringa, E.C., Koolwijk, P., and van Hinsbergh, V.W.M. (2021). Empagliflozin restores chronic kidney disease–induced impairment of endothelial regulation of cardiomyocyte relaxation and contraction. Kidney International. 10.1016/j.kint.2020.12.013.
79. Robinson, M.D., McCarthy, D.J., and Smyth, G.K. (2010). edgeR: a Bioconductor package for differential expression analysis of digital gene expression data. Bioinformatics *26*, 139–140. 10.1093/bioinformatics/btp616.
80. Ritchie, M.E., Phipson, B., Wu, D.I., Hu, Y., Law, C.W., Shi, W., and Smyth, G.K. (2015). limma powers differential expression analyses for RNA-sequencing and microarray studies. Nucleic acids research *43*, e47. 10.1093/nar/gkv007.
81. Law, C.W., Chen, Y., Shi, W., and Smyth, G.K. (2014). voom: Precision weights unlock

947 linear model analysis tools for RNA-seq read counts. Genome biology *15*, R29.
948 10.1186/gb-2014-15-2-r29.
949

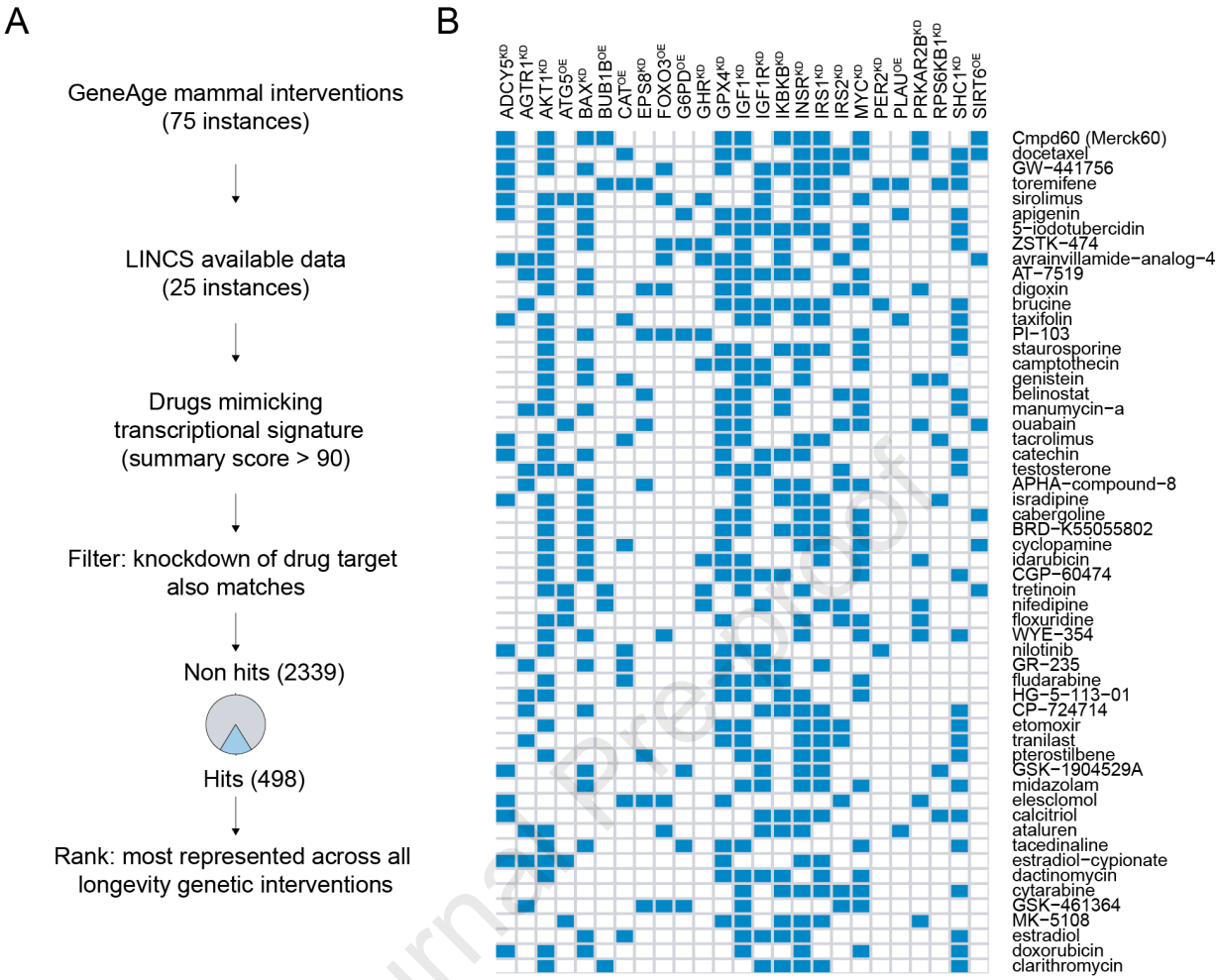

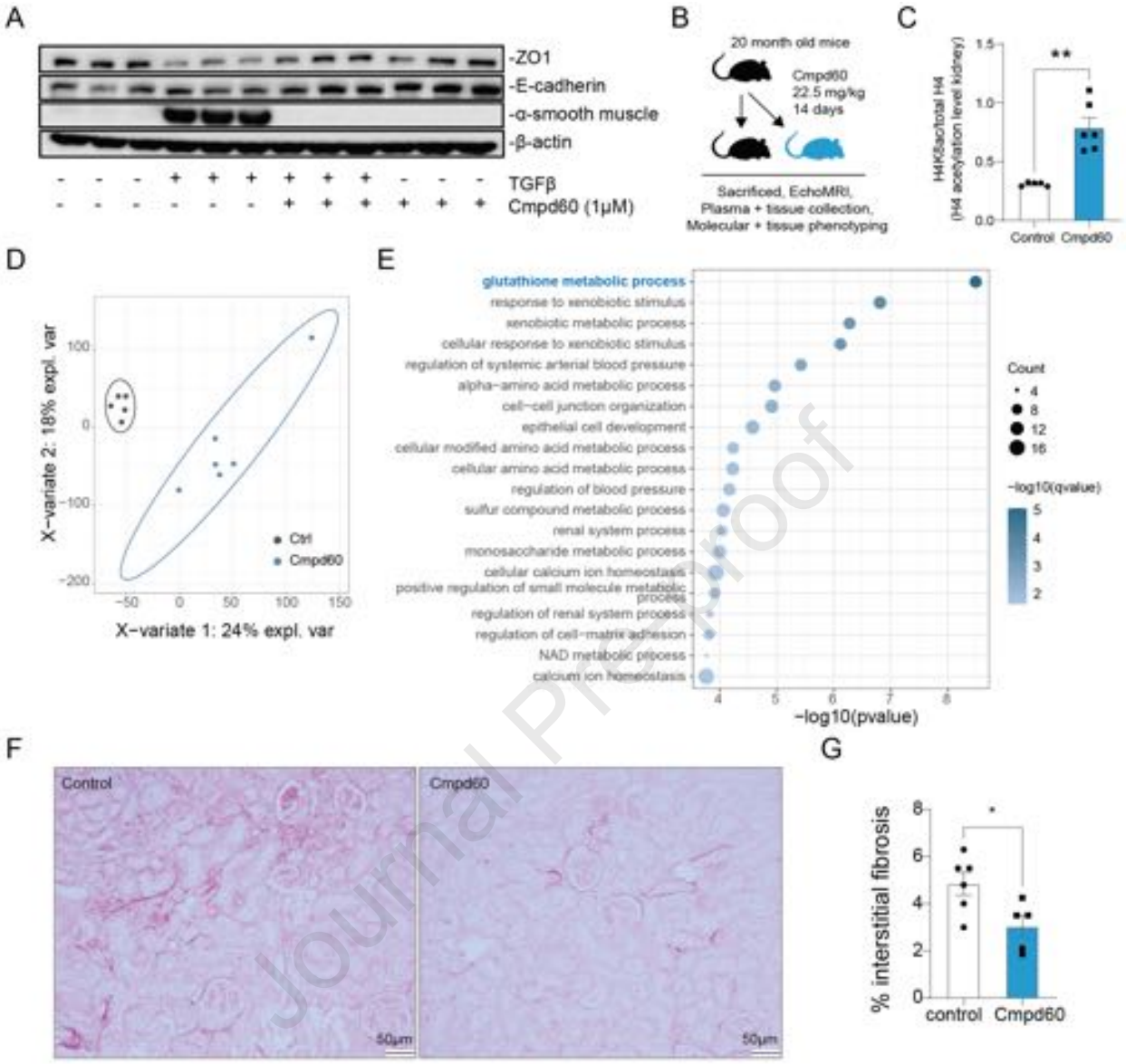

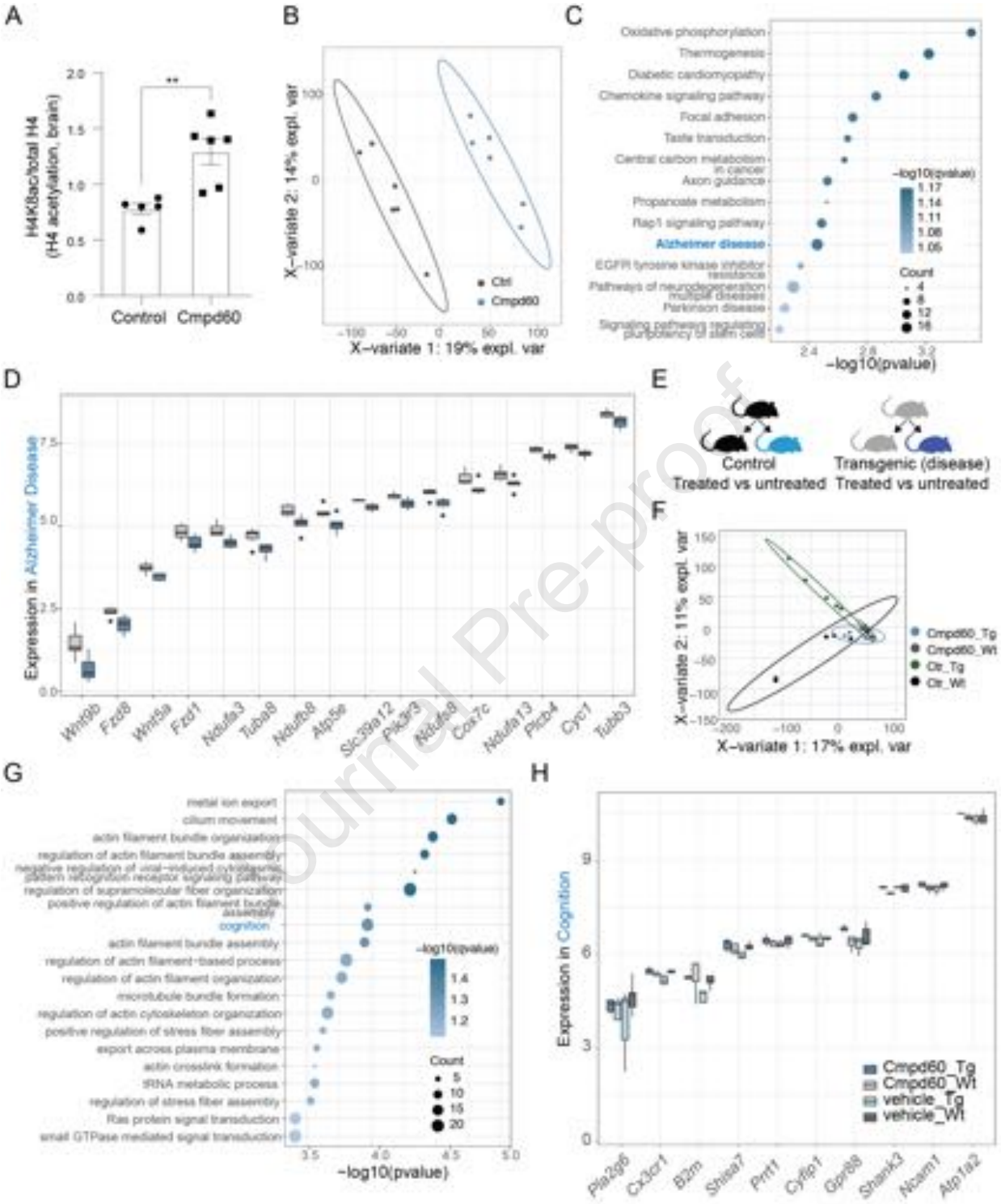

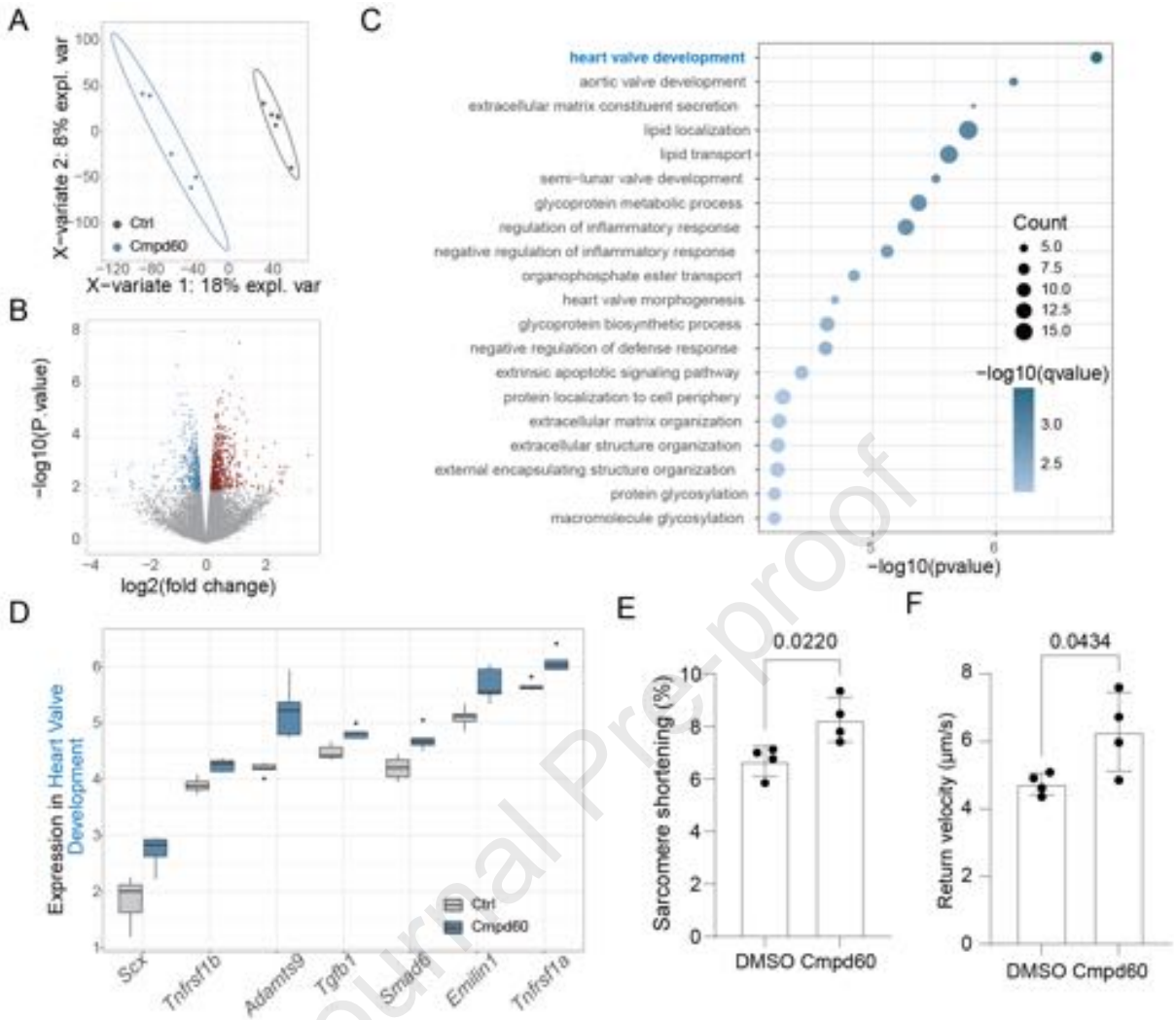

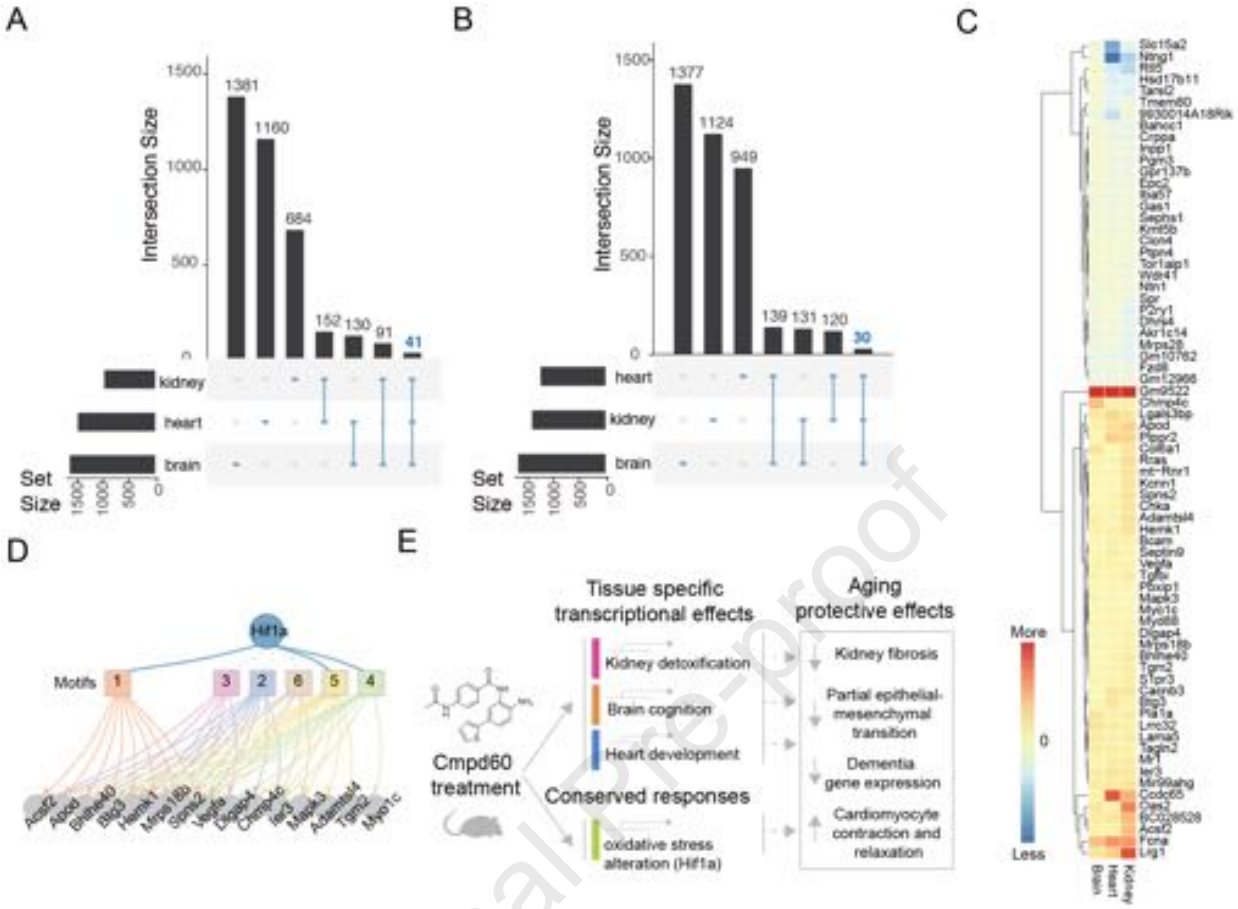

Highlights

- Transcriptome-based drug discovery finds compounds mimicking longevity interventions. Top candidate Cmpd60 reduces age-related phenotypes in multiple organs in mice.
- Renal aging: Cmpd60 curtails epithelial-mesenchymal transition and fibrosis.
- Brain aging: Cmpd60 diminishes dementia-related gene expression.
- Cardiac aging: Cmpd60 enhances ventricular contractility.